

## Logic gates based in two- and three-modes nonlinear optical fiber couplers

J. W. M. Menezes · W. B. de Fraga · A. C. Ferreira ·  
K. D. A. Saboia · A. F. G. F. Filho · G. F. Guimarães ·  
J. R. R. Sousa · H. H. B. Rocha · A. S. B. Sombra

Received: 12 April 2007 / Accepted: 24 January 2008 / Published online: 23 February 2008  
© Springer Science+Business Media, LLC. 2008

**Abstract** In this paper we did a study of logic gates obtained in the operation of a three-core non linear directional coupler (TNLDC) and an asymmetric two-core coupler (DNLDC) operating in the CW regime (the laser signals have the same wavelength). The symmetric three-core coupler (TNLDC), with their cores identical, in a planar arrangement, was studied using a control pulse applied to the first core. The second structure is an asymmetric two-core coupler (DNLDC). Looking at the transmission characteristics of the device, through the direct and cross channel, we did a study of the extinction ratio (Xratio) of these devices. For both devices we did a numerical investigation with the objective to implement logic gates. The DNLDC supplied AND, OR and XOR gates while the TNLDC supplied AND, NAND, OR, XOR and NOT gates. In comparing the performance of both switches operating as logic gates (DNLDC and TNLDC) we define, for the first time, a figure-of-merit of the logic gates (FOMELG). In this criteria the FOMELG is defined as a function of the extinction ratio of the gate outputs. Comparing the same gates of the three and two-core NLDC we observe that the logical gates of the three-core TNLDC present a better performance than the one of the two-core DNLDC considering the figure of merit FOMELG, besides the fact that is simpler to fabricate a symmetrical coupler (with identical cores) comparing with an asymmetric coupler. We believe that the use of this figure of merit will be useful in the study of the performance of logic gates to be used in communication systems.

**Keywords** Logic gates · Optical waveguide

---

J. W. M. Menezes · W. B. de Fraga · A. C. Ferreira · K. D. A. Saboia · A. F. G. F. Filho · G. F. Guimarães ·  
J. R. R. Sousa · H. H. B. Rocha · A. S. B. Sombra (✉)  
Laboratório de Telecomunicações e Ciência e Engenharia de Materiais LOCEM, Departamento de Física,  
Universidade Federal do Ceará, Caixa Postal 6030, Fortaleza, Ceará, 60455-760, Brazil  
e-mail: [sombra@fisica.ufc.br](mailto:sombra@fisica.ufc.br); [sombra@ufc.br](mailto:sombra@ufc.br)  
URL: [www.locem.ufc.br](http://www.locem.ufc.br)

A. C. Ferreira · A. F. G. F. Filho · G. F. Guimarães · H. H. B. Rocha  
Departamento de Engenharia de Teleinformática (DETI), Centro de Tecnologia, Universidade Federal  
do Ceará, Fortaleza, Ceará, 60455-760, Brazil

## 1 Introduction

Optical glasses have a number of advantages as nonlinear materials for all-optical devices. Their high transparency permits long interaction lengths in guided-wave structures and essentially eliminates the thermal heating problems that have affected the performance of all-optical devices made from semiconductor and nonlinear organic materials (Friberg and Smith 1987).

The interest that telecommunications companies have shown in increasing the data transmission capacity in their networks and the recent advances at the photonic device level it has generated intense research effort on ultrafast, nonlinear, all-optical switching devices. One reason for the current upsurge of interest in photonic switching has been the realization that all-optical devices have the capability to switch at rates much higher than those possible with electronics technology. Such high rates are likely to be necessary in future high-speed communications and computing systems (Smith 1984).

Several all-optical switching devices have been proposed and analyzed in the literature (Valkering et al. 1998, 1999; Chu et al. 1993, 1995; Agrawal 2001; Jensen 1982; Trillo et al. 1988; Kitayama and Wang 1983; Kivshar 1993; Akhmediev and Ankiewicz 1993, 1997; Akhmediev and Soto-Crespo 1994; Weiner et al. 1989; Chiang 1997a,b; Shum et al. 1999; Ramos and Paiva 1999) and the phenomenon of nonlinear directional coupling have been widely investigated for applications to all-optical ultrafast switching (Betts et al. 1991; Zang and Forest 1992; Sombra 1992; Chen et al. 1992; Nobrega and Sombra 1998; Castro et al. 2003; Buah et al. 1997; Donnelly et al. 1983; Deering et al. 1993; Atai and Malomed 2003; Griffin et al. 1991; Friberg et al. 1988; Kaup et al. 1997; Mak et al. 1998; Malomed et al. 1996; Lopez et al. 1994), the possibility of performing all classical logic operations by purely optical means (Wang and Liu 1999; Fraga et al. 2006; Trivunac-Vukovic and Milovanovic 2001; Trivunac-Vukovic 2001; Yang 1991; Yang and Wang 1992).

Directional fiber couplers constitute an essential component of a lightwave system. They are used routinely for a multitude of fiber-optic devices that require splitting of an optical field into two coherent but physically separated parts and vice versa. Fiber couplers are called symmetric when their cores are identical in all parameters. Switching is the process of energy redistribution among the cores for a given input. Since the transmission characteristics of this device are determined by the input power of the signal, by increasing the input power above a critical level the input signal can be switched from one core to other depending on the coupler length.

A two-core nonlinear directional fiber coupler (DNLDC) consists (see Fig. 1b), of two closely spaced, parallel, single mode waveguides constructed from a material with an intensity dependent index of refraction. At low light levels, the device behaves as a linear directional coupler. Because of evanescent coupling, signals introduced into channel 1 (direct channel) transfer completely to channel 2 (cross channel) in one coupler length  $L_c$ . Higher intensities induce changes in the refractive index and detune the coupler. Coupler is inhibited for input powers above the critical power:

$$P_C = \frac{A\lambda}{n_2 L_C} \quad (1)$$

where  $A$  is the effective mode area,  $\lambda$  is the pump wavelength and  $n_2$  is the nonlinear refractive index (Jensen 1982; Trillo et al. 1988; Kitayama and Wang 1983),  $L_C$  is the half-beat-length of the coupler, where  $L_C = \pi/2K$  for the two-core DNLDC and  $L_C = \pi/\sqrt{2}K$  ( $K$  is the linear coupling coefficient between adjacent guides,  $K = 0.3312 \text{ m}^{-1}$  for our numerical simulations) for the three core TNLDC. For the TNLDC (see Fig. 1a) we have a symmetric

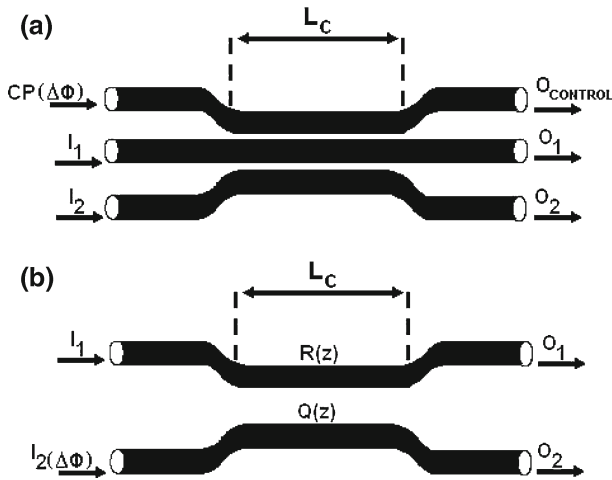


**Fig. 1** (a) Schematic of three-core TNLDC of length  $L_C$ . (b) Schematic of two-core DNLDC of length  $L_C$

coupler, composed of three guides. Under these conditions we are assuming coupling length ( $L_C$ ) around 4.74 m for two-core coupler and 6.70 m for three-core coupler.

Lossless device is an idealized situation. In practice, large or small, material loss is unavoidable, especially when nonlinearities are based on absorptive process in semiconductors. The absorption, uniformly distributed over the device, will set a limit to the operation of the device (Chen et al. 1992). In Nobrega and Sombra (1998) we did a study on the symmetric nonlinear directional (double core) coupler with loss. The presence of loss is responsible for the increase of the critical power of the coupler and a strong deformation of the nonlinear transmission of the device. We have investigated the effect of the self phase modulation profile (SPM) on the performance of an increasing self phase modulation (SPM) profile coupler. We have shown that appropriate shaping of the nonlinear SPM profile is quite effective to recover, almost completely, the original switching behavior associated to the lossless situation.

In this paper, we compare the performance of an asymmetric two-core DNLDC with a symmetric three core TNLDC operating in the CW regime. The performance was studied in view of the possible use of these devices as logic gates in optical networks. A new figure of merit, will be defined, and used to compare the performance of these devices.

## 2 Theoretical framework

For the symmetric three-core TNLDC (Fig. 1a), the cores are assumed to be the same with the nonlinearity in the fiber described by the Kerr effect, and neglecting high order dispersion and loss. This device is constituted of three cores, where those channels can be used as input and output. Previous studies have demonstrated that the three-core TNLDC offers some advantages over the usual two-waveguide coupler as described by Jensen. These studies indicate, by comparison with the two wave-guide coupler, that the  $n$ -wave-guide couplers ( $n > 2$ ) have more output states, with sharper switches characteristics, and display greater sensitivity to the input state, which are very important characteristics for the all optical switching schemes proposed (Stegeman and Wright 1990; Da Silva and Sombra 1998). The price for the improvement in the switching is however, the growth of the critical potency. The three-core

nonlinear fiber coupler in a parallel arrangement is described by the coupled NLSE'S (2–4), where considered that the interactions between the cores 1 and 3 are worthless, only existing joining between the neighboring closer cores. Thus,

$$-i \frac{du_1}{dz} = R(z) |u_1|^2 u_1 + Ku_2 \tag{2}$$

$$-i \frac{du_2}{dz} = R(z) |u_2|^2 u_2 + K(u_1 + u_3) \tag{3}$$

$$-i \frac{du_3}{dz} = R(z) |u_3|^2 u_3 + Ku_2 \tag{4}$$

where  $K$  is the linear coupling coefficient between adjacent guides and  $R(z) = 0.25 W^{-1} m^{-1}$  is the SPM profile.

For the asymmetric DNLDC (Fig. 1b), the nonlinearity is a function of the  $z$  coordinate only in channel 2. For the sake of convenience we neglect the weak nonlinear cross-phase modulation (XPM). The coupled differential equations describing the evolution of the slowly varying complex modal amplitudes  $u_v$  of the aligned two-core coupler are:

$$-i \frac{du_1}{dz} = R(z) |u_1|^2 u_1 + Ku_2 \tag{5}$$

$$-i \frac{du_2}{dz} = Q(z) |u_2|^2 u_2 + Ku_1 \tag{6}$$

where  $K$  is the linear coupling coefficient between adjacent guides,  $R(z) = 1 W^{-1} m^{-1}$  and  $Q$  the SPM profile, which is proportional to the nonlinear refractive index  $n_2$  (Jensen 1982; Trillo et al. 1988; Kitayama and Wang 1983):

$$Q = \pm \frac{4K}{P_C} = \pm \frac{4Kn_2L_C}{A\lambda} \tag{7}$$

for the Kerr-law nonlinearity with  $+$  designating self-focusing materials, and  $P_C$  is the critical power defined before. A large number of studies have been trying to quantify the nonlinear refractive index  $n_2$ . It was found a relation between the nonlinear index of refraction  $n_2$ , the linear index of refraction  $n_0$  and the Abbe number  $\nu$ . Recently, using the bond orbital concept the following equation was obtained (Boling et al. 1978; Lines 1991):

$$n_2 = \frac{Z(n_0^2 - 1)d^2}{n_0 E_s^2} 10^{-16} \left( \frac{cm^2}{W} \right) \tag{8}$$

where  $Z$  is the cation's valence,  $d$  is the bond length and  $E_s$  is the Sellmeier gap (mean energy difference between valence and conduction band) valid to crystalline system.

In this paper, we do a study of the asymmetric coupler, where one of the guides present an increasing SPM profile ( $Q(z)$ ) where the first guide remains constant ( $R(z)=1$ ). We will study two simple coefficient of SPM profiles, for the DNLDC, namely constant and linear (increasing and decreasing). These profiles expressed in terms of the parameters  $\beta$ (maximum value of  $Q$ ) and  $L$  (length of the coupler) are:

$$Q(z) = \left( \frac{\beta - 1}{L} z + 1 \right) \text{ Linear} \tag{9}$$

$$Q(z) = \beta \text{ Constant} \tag{10}$$

Note that in these normalized SPM profiles the coefficient  $Q(z)$  monotonically increases from 1 to a final value of  $\beta$ , after a length  $L$  of the coupler. For the constant profile (Eq. 10) there is no variation along the coupler.

### 3 Numerical procedure

We have analyzed numerically the signal transmission through the two-core, DNLDC (Eqs. 5 and 6) with profile given by Eq. 7 and the three-core, TNLDC (Eqs. 2–4) nonlinear directional fiber coupler. For the DNLDC, the initial pulse at the input core is given by:

$$u_1(0, \tau) = A_i \quad (11)$$

$$u_2(0, \tau) = B_i \exp(i \Delta \phi) \quad (12)$$

where  $\Delta \phi$  is the dephasing between the two input lasers.

For the TNLDC, the initial pulse at the input core is given by:

$$u_1(0, \tau) = A_i \exp(i \Delta \phi) \quad \text{control signal (CP)} \quad (13)$$

$$u_2(0, \tau) = B_i \quad (14)$$

$$u_3(0, \tau) = C_i \quad (15)$$

where  $\Delta \phi$  is the signal applied to the first core that plays the role of a control signal (CP), that we can assume value “1” (with a phase difference of  $\Delta \Phi = \Delta \theta \pi$  between the inputs  $I_1$  and  $I_2$ ) or “0”, depending on the need of obtaining a certain logic gate. The inputs  $I_1$  and  $I_2$  are excited in agreement with a sequence of combinations (0;0), (0;1), (1;0), (1;1). In accordance with the signals of the outputs  $O_1$  and  $O_2$ , we calculate the Extinction Ratio (dB). In this paper the Extinction Ratio is represented as XR1 (for  $O_1$  output) and XR2 (for  $O_2$  output). For the TNLDC the sign “1” applied the control signal (CP) and the inputs  $I_1$  and  $I_2$  refer to a pump power of 1 W.

These systems of linearly coupled (Eqs. 2–4) was solved numerically using the fourth order Runge–Kutta method with 1,024 temporal grid points taking in account the initial conditions given by Eqs. 13–15.

We can define the transmission  $T_i$  as a function of the signal energies:

$$T_i = \frac{\int_{-\infty}^{+\infty} |u_i(L_C)|^2 dt}{\int_{-\infty}^{+\infty} |u_i(0)|^2 dt} \quad (16)$$

With  $i=1, 2$  for DNLDC and  $i=1, 2, 3$  for the TNLDC with length of  $L_C$ .

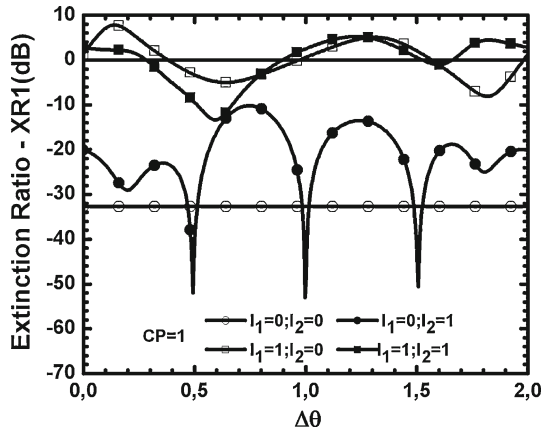
The extinction ratio of an on-off switch is the ratio of the output power in the on state to the output power in the off state. This ratio should be as high as possible. For our NLDC it is expressed by:

$$\text{Extinction - ratio} = X(R) = \frac{\int_{-\infty}^{+\infty} |u_1(L_C)|^2 dt}{\int_{-\infty}^{+\infty} |u_2(L_C)|^2 dt} \quad (17)$$

where the extinction ratio in dB units is:

$$\text{Extinction - ratio [dB]} = X_{\text{ratio}} = XR = 10 \log_{10} X(R) \quad (18)$$

**Fig. 2** Xratio level for the symmetrical three-core TNLDC as a function of the  $\Delta\Phi = \Delta\theta\pi$  parameter, obtained from the numerical solution of Eqs. 2–4 with  $CP=1(\Delta\Phi)$ ,  $(I_1; I_2) = [(0; 0); (0; 1); (1; 0); (1; 1)]$ ,  $K=0.3312$ ,  $L_C = \pi/\sqrt{2}K$ ,  $R(z)=0.25$



### 4 Results and discussion

In Fig. 2 we have the extinction ratio results concerning the configuration where  $CP = 1(\Delta\Phi)$  and the input signals are pulses in sequences of (0;0), (0;1), (1;0), (1;1). For the TNLDC with  $CP = 1(\Delta\Phi)$  and the inputs  $(I_1; I_2) = (0; 0)$  we have that, for any phase  $\Delta\Phi$  applied to the control pulse (CP), the extinction ratio ( $O_1/O_2$ ) is around  $-32$  dB. It means that 99.87% of the output energy in the control signal is switched for the  $O_2$  output.

In Fig. 2 we have the extinction ratio results concerning the configuration where  $CP=1(\Delta\Phi)$  and  $(I_1; I_2) = (0; 1)$ . We can notice that the values of  $XR1(\text{dB})$  is always negative for any variation of  $\Delta\Phi = \Delta\theta\pi$ , with strong fluctuations. It means that the switched energy is alternating between  $O_2$  and  $O_1$  outputs. However the majority of the power is present in  $O_2$  channel. At the dephasing values around  $\Delta\Phi = 0.493\pi$ ,  $\Delta\Phi = 0.998\pi$  and  $\Delta\Phi = 1.507\pi$ , we have the Xratio around  $-51.86$  dB. It means that for this input dephasing the switched signal is predominantly in  $O_2$ . For  $CP=1(\Delta\Phi)$  and  $(I_1; I_2) = (1; 0)$  we verify that the values of  $XR1(\text{dB})$  are alternated (some times positive and negative). This behavior is due to the fact that in this condition practically all the energy is transferred periodically between  $O_1$  and  $O_2$  outputs, being a small fraction of this energy present in  $O_{\text{CONTROL}}$  (output control). The largest intensities for  $XR1(\text{dB})$  are reached when  $\Delta\Phi = 0.140\pi$ , and  $\Delta\Phi = 1.819\pi$  with  $7.80$  dB. For  $\Delta\Phi = 0.380\pi$ ,  $\Delta\Phi = 0.973\pi$  and  $\Delta\Phi = 1.567\pi$  the fractions of energy in the  $O_1$  and  $O_2$  outputs are identical, providing null values for  $XR1(\text{dB})$  and  $XR2(\text{dB})$ . For  $CP=1(\Delta\Phi)$  and  $(I_1; I_2)=(1;1)$ , for  $\Delta\Phi = 0.585\pi$ , we have the largest intensity, in module (around  $13.28$  dB), for  $XR1(\text{dB})$ . For this configuration,  $O_2$  and  $O_1$  have a low fraction of energy and the largest portion of the energy is in the  $O_{\text{CONTROL}}$  (output control). For  $\Delta\Phi = 0.280\pi$ ,  $\Delta\Phi = 0.897\pi$ ,  $\Delta\Phi = 1.523\pi$  and  $\Delta\Phi = 1.663\pi$  the fractions of energy in the  $O_1$  and  $O_2$  outputs are identical, providing null values for  $XR1(\text{dB})$ .

Table 1 shows the values of  $XR1(\text{dB})$  and  $XR2(\text{dB})$  as well as the fraction of switched energy for all configurations.

In the configuration where  $CP=0$  and the inputs  $(I_1; I_2) = (0; 0)$ , we have for the three-core TNLDC the trivial solution. The phase  $\Delta\Phi$  does not have any influence in the operation of the logic gate, Thus the outputs  $XR1(\text{dB})$  and  $XR2(\text{dB})$  always present a constant value (see Tables 1 and 2).

To implement the logic gates we select the phases  $\Delta\Phi = 1.81\pi$  and  $\Delta\Phi = 0.63\pi$ , with  $CP=0$  or  $CP=1$ , as we can verify in Tables 1 and 2. For the first case (Table 1), with

**Table 1** Symmetric couplers operating with CP=0 or CP=1 ( $\Delta\phi = 1.81\pi$ ) for a coupler length of  $L_C = 6.70$

$I_1$		$I_2$		$\Delta\phi = 1.81\pi$									
$I_1$	$I_2$	CP $\Delta\phi$	O <sub>1</sub> XR <sub>1</sub> (dB)	O <sub>2</sub> XR <sub>2</sub> (dB)	CP $\Delta\phi$	O <sub>1</sub> XR <sub>1</sub> (dB)	O <sub>2</sub> XR <sub>2</sub> (dB)	CP $\Delta\phi$	O <sub>1</sub> XR <sub>1</sub> (dB)	O <sub>2</sub> XR <sub>2</sub> (dB)	CP $\Delta\phi$	O <sub>1</sub> XR <sub>1</sub> (dB)	O <sub>2</sub> XR <sub>2</sub> (dB)
0	0	1	(0.000537) -32.69 dB	(0.99875) +32.69 dB	0	0	0	1	(0.000537) -32.69 dB	(0.99875) +32.69 dB	1	(0.000537) -32.69 dB	(0.99875) +32.69 dB
			0	1		0	1		0	1		0	1
0	1	1	(0.00184) -24.98 dB	(0.57940) +24.98 dB	1	(0.00184) -24.98 dB	(0.57940) +24.98 dB	1	(0.00184) -24.98 dB	(0.57940) +24.98 dB	1	(0.00184) -24.98 dB	(0.57940) +24.98 dB
			0	1		0	1		0	1		0	1
1	0	1	(0.26987) -8.06 dB	(1.7269) +8.06 dB	1	(0.26987) -8.06 dB	(1.7269) +8.06 dB	1	(0.26987) -8.06 dB	(1.7269) +8.06 dB	1	(0.26987) -8.06 dB	(1.7269) +8.06 dB
			0	1		0	1		0	1		0	1
1	1	0	(1.13794) +37.27 dB	(0.000213) -37.27 dB	0	(1.13794) +37.27 dB	(0.000213) -37.27 dB	1	(1.13794) +37.27 dB	(0.000213) -37.27 dB	1	(1.13794) +37.27 dB	(0.000213) -37.27 dB
			1	0		1	0		1	0		1	0
			AND Gate	NAND Gate		AND Gate	XOR Gate		AND Gate	NOT Gate		AND Gate	NAND Gate

The output  $O_2^{(*)}$  is related with the input  $I_1$

**Table 2** Symmetric couplers operating with CP=0 or CP=1( $\Delta\phi = 0.63\pi$ ) for a coupler length of  $L_C = 6.70$

$I_1$	$I_2$	$\Delta\phi = 0.63\pi$	CP $\Delta\phi$	$O_1$ XR <sub>1</sub> (dB)	$O_2$ XR <sub>2</sub> (dB)	CP $\Delta\phi$	$O_1$ XR <sub>1</sub> (dB)	$O_2$ XR <sub>2</sub> (dB)	CP $\Delta\phi$	$O_1$ XR <sub>1</sub> (dB)	$O_2$ XR <sub>2</sub> (dB)	CP $\Delta\phi$	$O_1$ XR <sub>1</sub> (dB)	$O_2$ XR <sub>2</sub> (dB)
0	0	1	0	(0.000537) -32.69 dB 0	(0.99875) +32.69 dB 1	0	(0.000537) -32.69 dB 0	(0.99875) +32.69 dB 1	0	(0.000537) -32.69 dB 0	(0.99875) +32.69 dB 1	0	(0.000537) -32.69 dB 0	(0.99875) +32.69 dB 1
0	1	1	1	(0.03127) -13.55 dB 0	(0.70975) +13.55 dB 1	1	(0.03127) -13.55 dB 0	(0.70975) +13.55 dB 1	1	(0.03127) -13.55 dB 0	(0.70975) +13.55 dB 1	1	(0.03127) -13.55 dB 0	(0.70975) +13.55 dB 1
1	0	1	1	(0.47696) -4.99 dB 0	(1.50565) +4.99 dB 1	1	(0.47696) -4.99 dB 0	(1.50565) +4.99 dB 1	1	(0.47696) -4.99 dB 0	(1.50565) +4.99 dB 1	1	(0.47696) -4.99 dB 0	(1.50565) +4.99 dB 1
1	1	0	0	(1.13794) +37.27 dB 1	(0.000213) -37.27 dB 0	0	(1.13794) +37.27 dB 1	(0.000213) -37.27 dB 0	0	(1.13794) +37.27 dB 1	(0.000213) -37.27 dB 0	0	(1.13794) +37.27 dB 1	(0.000213) -37.27 dB 0
				AND Gate	NAND Gate			OR Gate			NOT Gate		AND Gate	XOR Gate

The output  $O_2^{(*)}$  is related with the input  $I_1$



$\Delta\Phi = 1.81\pi$  we implemented the AND, NAND, XOR and NOT logical gates and for the second case, Table 2, with  $\Delta\Phi = 0.63\pi$ , one can notice the operation of AND, NAND, OR, XOR and NOT logical gates.

Considering all the studied configurations in Tables 1 and 2, we can conclude that the logic gates AND, XOR, OR and NAND and NOT were obtained. In our analysis we can look for the extinction ratio to have an exact view of the performance of the logic gate. In Table 1 we have three possibilities to have the AND gate. The signal inputs  $I_1$  and  $I_2$  are the same. However the control signal was modified. For the sequence of the input signals (00),(01),(10) and (11) we choose four different configurations for the control pulse CP (column values in Table 1): (1,1,1,0), (0,1,1,0), (1,1,0,0) and (1,1,1,1). All these three possibilities are leading for three different AND gates (see Table 1). In comparing the three logic gates, we choose to create a figure of merit defined as a function of the extinction ratio of the gate outputs. We will look for the sum of the module values of the extinction ratio (XR) for each output of the logic gate. In this criteria we choose to not consider the trivial condition, where the input is (00) and the gate output is also 0. Which it is the case for AND, XOR and OR gates. For gates where for the input (00) we have output 1, will be taken in the value of the FOMELG parameter:

$$\text{FOMELG (dB)} = |XR(1, 0)| + |XR(0, 1)| + |XR(1, 1)| \quad (19)$$

$$\text{FOMELG (dB)} = |XR(0, 0)| + |XR(1, 0)| + |XR(0, 1)| + |XR(1, 1)| \quad (20)$$

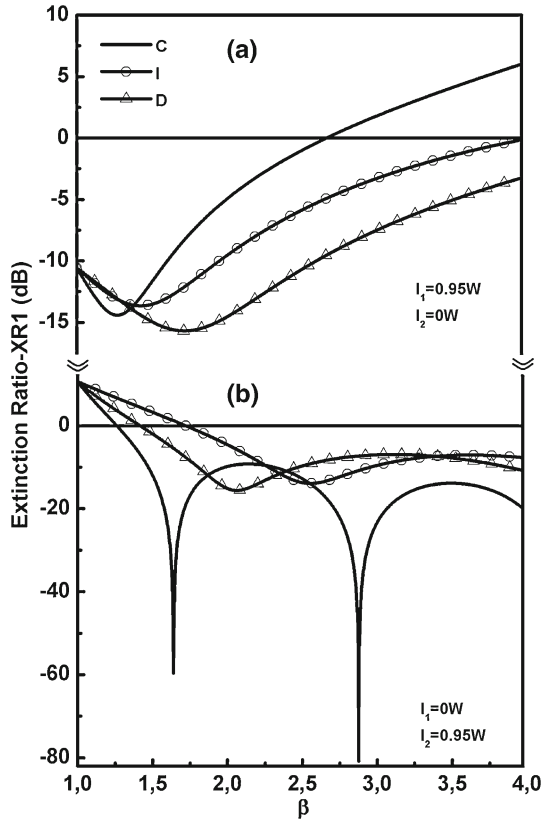
for gates with and without the trivial configuration respectively.

Looking now for the three AND gates in Table 1, we can say that the value for the FOMELG parameter will be 70.31, 70.31 and 37.47 dB. One can say that the first two configurations of the AND gate are equivalent and present better behavior compared to the third one. This criteria will be useful in comparing the performance of the double and triple couplers.

For DNDLC (two-core coupler) we have the extinction ratio measured with the incident power present in input 1 ( $u_2 = 0$ ). In this configuration we are looking for the dependence of the Xratio as function of the final value of the nonlinear profile  $\beta$ . In this study three different couplers were examined. In the first one (C) the asymmetric coupler is composed of two guides: guide 1( $R(z)=1$ ) and guide 2( $Q(z)$ ) with the higher nonlinearity. For this guide the profile is constant with value  $Q(z)=\beta$ . In the second case (I) one has an increasing profile (Eq. 9) where the nonlinearity increases from 1 to the final value  $\beta$ . In the last coupler (D) one has a decreasing profile where at the beginning of the coupler the value of the nonlinearity is  $\beta$  and decreases to 1 at the end of the coupler. It is equivalent to the sample coupler discussed before, however the pump laser is incident in the output of the fiber ( $O_1$ , see Fig. 1a).

In Fig. 3a, we have a pump power incident in channel 1 ( $I_1=0.95$  W). One can notice that for  $\beta = 1$  all the couplers present the same Xratio value around  $-10.5$  dB. It means that all the light is switched to port 2 of the coupler ( $O_2$ ). With the increase of the nonlinearity we can notice that for all the couplers the Xratio is decreasing with the lowest value obtained for the decreasing profile (D) with  $Xratio=-15.68$  dB around  $\beta \approx 1.74$ . With the increase of the  $\beta$  value one has an increase of the Xratio value. It means that the light is switching back to first guide. In Fig. 3b, one has the Xratio study for the same incident light, pumping now in channel 2 ( $I_2$ ). In this configuration for  $\beta = 1$ , the output light is present in channel 1 ( $O_1$ ). The Xratio is positive with value around 10.61 dB. However with the increase of the  $\beta$  value the Xratio value start decreasing indicating that the light is switching back to channel 2. All the couplers present a minimum in the Xratio value (see Fig. 3a). For the constant profile this minimum is around  $Xratio \approx -59.57$  dB for  $\beta \approx 1.63$ . For the decreasing (D) and increasing (I) couplers the  $Xratio \approx -15.58$  dB for  $\beta = 2.06$  and  $Xratio \approx -13.88$  dB for  $\beta = 2.55$ .

**Fig. 3** (a) Xratio level of the couplers C,I, and D (DNLDC) as a function of the  $\beta$  parameter, obtained from the numerical solution of Eqs. 5 and 6 together with Eqs. 9 and 10 with  $I_1=0.95\text{ W}$ ,  $K=0.3312$ ,  $L_C = \pi/2K$ ,  $Q(z)$ ,  $R(z)=1$ . (b) Xratio level of the couplers C,I, and D as a function of the  $\beta$  parameter, obtained from the numerical solution of Eqs. 5 and 6 together with Eqs. 9 and 10 with  $I_2=0.95\text{ W}$ ,  $K=0.3312$ ,  $L_C = \pi/2K$ ,  $Q(z)$ ,  $R(z)=1$

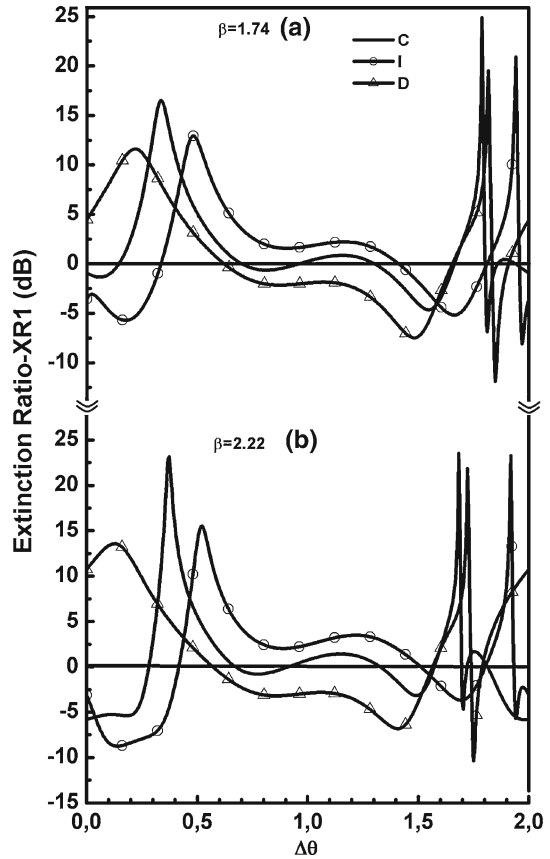


Considering these two input situations (1,0) and (0,1) one has to choose now the configuration of the (1,1) in trying to implement the logic operation. Considering the best performance of these two configurations one choose two values for the  $\beta$  parameter: 1.74 and 2.22. As suggested by others authors we explore the situation where both input channel were excited (see Fig. 1b) considering a phase difference between these two pulses (see Eqs. 2 and 3).

In Fig. 4a, we have the Xratio of the same couplers considering  $\beta = 1.74$  with  $I_1 = I_2 = 0.95\text{ W}$  and a phase difference of  $\Delta\phi = \Delta\theta\pi$ . It is clear that for  $\Delta\theta = 0$  the incident signals are switched between the two guides with stronger presence of light in guide 1 (D coupler) and guide 2 (I and C couplers). With the increase of the dephasing value ( $\Delta\phi$ ) the Xratio is increasing for all the couplers with maximum value of (+16.50 dB) obtained for the constant profile ( $\Delta\phi = 0.34\pi$ ). For the I and D couplers the values were around +12.92 dB at  $\Delta\phi = 0.48\pi$ ) and +11.60 dB at  $\Delta\phi = 0.21\pi$  respectively. With the increase of the dephasing value one has an inversion of the switching behavior. The majority of the power is switched for channel 2 (see Fig. 4a). The higher level of inversion is obtained for the D coupler (-11.95 dB at  $\Delta\phi = 1.85\pi$ ). In Fig. 4b, one has the same study, however considering  $\beta = 2.22$ . This value is associated to second higher Xratio observed for pump in channel 2.

The Xratio of the same couplers considering  $\beta = 2.22$  with  $I_1 = I_2 = 0.95\text{ W}$  with a phase difference of  $\Delta\phi$  is shown in Fig. 4b. It is clear that for  $\Delta\phi = 0$  a stronger presence of light in guide 1 (D coupler) and guide 2 (C and I couplers) was observed (see Fig. 4b). With

**Fig. 4** (a) Xratio level of the couplers C,I, and D (DNLDC) as a function of the input energy ( $W$ ), obtained from the numerical solution of Eqs. 5 and 6 together with Eqs. 9 and 10 with  $I_1 = I_2 = 0.95 W$ ,  $\Delta\Phi = 0.34\pi$ ,  $\beta = 1.74$ ,  $K = 0.3312$ ,  $L_C = \pi/2K$ ,  $Q(z)$ ,  $R(z) = 1$ . (b) Xratio level of the couplers C,I, and D as a function of the input energy ( $W$ ), obtained from the numerical solution of Eqs. 5 and 6 together with Eqs. 9 and 10 with  $I_1 = I_2 = 0.95 W$ ,  $\Delta\Phi = 0.34\pi$ ,  $\beta = 2.22$ ,  $K = 0.3312$ ,  $L_C = \pi/2K$ ,  $Q(z)$ ,  $R(z) = 1$



the increase of the dephasing value ( $\Delta\phi$ ) the Xratio is increasing for two of the couplers with maximum value (+23.40 dB) obtained for the constant profile ( $\Delta\phi = 1.68\pi$ ). For the I and D couplers the values were around +15.72 dB at  $\Delta\phi = 0.51\pi$  and +13.60 dB at  $\Delta\phi = 0.12\pi$  respectively.

In Tables 3 and 4 one has a summary of the results considering the three couplers with different dephasing values ( $\Delta\phi = 0.34\pi$  and  $0.416\pi$ ),  $\beta = 1.74$  and  $2.22$  respectively and coupler length of  $L_C = 4.74$ .

In comparing the performance of both switches operating as logic gates (DNLDC and TNLDC) we will use the figure-of-merit of the logic gates (FOMELG).

In Table 5 we have the FOMELG parameter for the DNLDC and TNLDC obtained from Tables 1 to 4. Comparing the logic gates that present the trivial configuration, which are the AND, XOR and OR gates in our present case (see Eq. 19). For the DNLDC the best gate is the AND gate and XOR gate obtained for the constant profile with FOMELG = 42.18 dB. For the OR gate the FOMELG parameter is around 16.91 dB (increasing profile). However these values are well behind when compared to the FOMELG obtained from the TNLDC. The AND and XOR gates is around 70.31 dB. For the OR gate the TNLDC is presenting a value of FOMELG which is almost double (in dB units, 31.75 dB) the value presented by the DNLDC (16.91 dB). We can conclude that the three-core coupler (TNLDC) is presenting

**Table 3** Asymmetric couplers operating with  $(\Delta\phi = 0.34\pi)$ ,  $\beta = 1.74$  and coupler length of  $L_C = 4.74$

$I_1$	$I_2$	Constant (C)		Increasing (I)		Decreasing (D)	
		$O_1$ XR <sub>1</sub> (dB)	$O_2$ XR <sub>2</sub> (dB)	$O_1$ XR <sub>1</sub> (dB)	$O_2$ XR <sub>2</sub> (dB)	$O_1$ XR <sub>1</sub> (dB)	$O_2$ XR <sub>2</sub> (dB)
0	0	0 (0.134)	0 (0.865)	0 (0.060)	0 (0.940)	0 (0.026)	0 (0.974)
1	0	-8.10 dB 0	+8.10 dB 1	-11.95 dB 0	+11.95 dB 1	-15.74 dB 0	+15.74 dB 1
0	1	0 (0.017)	+17.61 dB 1	0 (0.481)	+0.33 dB 1	0 (0.132)	0 (0.869)
1	1 ( $\Delta\Phi = 0.34\pi$ )	-17.61 dB 0 (1.952)	-16.47 dB 0 (0.044)	-0.33 dB 1 (1.054)	+0.48 dB 1 (0.944)	-8.18 dB 0 (1.716)	+8.18 dB 1 (0.284)
		+16.47 dB 1 AND Gate (with gain)	-16.47 dB 0 XOR Gate	+0.48 dB 1 -	-0.48 dB 1 OR Gate	+7.81 dB 1 AND Gate (with gain)	-7.81 dB 0 XOR Gate

**Table 4** Asymmetric couplers operating with  $\Delta\phi = 0.416\pi$ ,  $\beta = 2.22$  and coupler length of  $L_C = 4.74$

$I_1$	$I_2$	Constant (C)		Increasing (I)		Decreasing (D)	
		$O_1$ XR <sub>1</sub> (dB)	$O_2$ XR <sub>2</sub> (dB)	$O_1$ XR <sub>1</sub> (dB)	$O_2$ XR <sub>2</sub> (dB)	$O_1$ XR <sub>1</sub> (dB)	$O_2$ XR <sub>2</sub> (dB)
0	0	0 (0.327)	0 (0.671)	0 (0.140)	0 (0.859)	0 (0.048)	0 (0.951)
1	0	-3.12 dB	+3.12 dB	-7.88 dB	+7.88 dB	-12.97 dB	+12.97 dB
		0	1	0	1	0	1
0	1	(0.103) -9.39 dB	(0.896) +9.39 dB	(0.113) -8.94 dB	(0.886) +8.94 dB	(0.041) -13.69 dB	(0.958) +13.69 dB
		0	1	0	1	0	1
1	1 ( $\Delta\Phi = 0.416\pi$ )	(1.888) +12.35 dB	(0.11) -12.35 dB	(1.01) +0.09 dB	(0.99) -0.09 dB	(1.414) +3.84 dB	(0.584) -3.84 dB
		1	0	1	1	1	0
		AND Gate (with gain)	XOR Gate	AND Gate	OR Gate	AND Gate (with gain)	XOR Gate

**Table 5** FOMELG parameter obtained from Tables 1 to 4 (see Eqs. 19 and 20)

Figure-of-merit of logic gates-FOMELG (dB)	Two core coupler DNLDC	Three core coupler TNLDC
AND	42.18 dB (C, $\Delta\phi = 0.34\pi$ )	70.31 dB ( $\Delta\phi = 1.81\pi$ )
	31.73 dB (D, $\Delta\phi = 0.34\pi$ )	55.81 dB ( $\Delta\phi = 0.63\pi$ )
	30.5 dB (D, $\Delta\phi = 0.416\pi$ )	37.47 dB ( $\Delta\phi = 1.81\pi$ )
	24.86 dB (D, $\Delta\phi = 0.416\pi$ )	
	16.91 dB (I, $\Delta\phi = 0.416\pi$ )	
XOR	42.18 dB (C, $\Delta\phi=0.34\pi$ )	70.31 dB ( $\Delta\phi = 1.81\pi$ )
	31.73 dB (D, $\Delta\phi = 0.34\pi$ )	55.81 dB ( $\Delta\phi = 0.63\pi$ )
	30.5 dB (D, $\Delta\phi = 0.416\pi$ )	
	24.86 dB (D, $\Delta\phi = 0.416\pi$ )	
OR	16.91 dB (I, $\Delta\phi = 0.416\pi$ )	31.75 dB ( $\Delta\phi = 0.63\pi$ )
	12.76 dB (I, $\Delta\phi = 0.34\pi$ )	
NAND		70.31 dB ( $\Delta\phi = 1.81\pi$ )
		55.81 dB ( $\Delta\phi = 0.63\pi$ )
NOT		37.47 dB ( $\Delta\phi = 1.81\pi$ )
		99.74 dB ( $\Delta\phi = 1.81\pi$ )
		88.31 dB ( $\Delta\phi = 0.63\pi$ )

better performance for the FOMELG parameter when compared to the two-core (DNLDC) device.

The TNLDC present two extra gates, NAND and NOT which is presenting values of FOMELG (without the trivial situation, see Eq. 20) of 70.31 and 99.74 dB respectively. These extra logic gates were not observed in the DNLDC switch.

## 5 Conclusion

A full set of logic functions including AND, NAND, XOR, NOT and OR gates are numerically demonstrated using a two-core (DNLDC) and three core (TNLDC) switches operating in the CW regime. We have shown that logic gates AND, OR and XOR can be constructed from an asymmetric two-core NLDC while the symmetrical three-core NLDC produced logical gates NAND, AND, OR, XOR and NOT.

For the TNLDC, the phase  $\Delta\Phi = 1.81\pi$ , generated more efficient logical gates than the phase  $\Delta\Phi = 0.63\pi$ , however the phase  $\Delta\Phi = 0.63\pi$  supplied a bigger number of logic gates where the logic gate OR is only implemented with this phase. With  $\Delta\Phi = 1.81\pi$ , the logical gates AND, NAND, XOR and NOT were implemented and with  $\Delta\Phi = 0.63\pi$  the logical gates AND, NAND, OR, XOR and NOT were obtained.

For the DNLDC the best performance for the logic gates AND and XOR were obtained for the constant profile (42.18 dB for both gates) compared to the D and I couplers (for  $\beta = 1.74$ , see also Table 5). For  $\beta = 2.22$  the I coupler presents the best performance for OR logic gate. The OR logic gate is only implemented in the I coupler (increasing profile coupler).

In comparing the performance of both switches operating as logic gates (DNLDC and TNLDC) we will use the figure-of-merit of the logic gates (FOMELG).

In this criteria the FOMELG is defined as a function of the extinction ratio of the gate outputs. We will look for the sum of the module values of the extinction ratio (XR) for each output of the logic gate. We choose to not consider the trivial condition where the input is (00) and the gate output is also 0. Comparing the logic gates that they present the trivial

configuration, which are the AND, XOR and OR gates in our present case (see Eq. 19). For the DNLDC the best gate is the AND gate and XOR gate obtained for the constant profile with FOMELG=42.18 dB. For the OR gate the FOMELG parameter is around 16.91 dB (increasing profile). However these values are well behind when compared to the FOMELG obtained from the TNLDC. The AND and XOR gates is around 70.31 dB. For the OR gate the TNLDC is presenting a value of FOMELG which is almost double (31.75 dB) the value presented by the DNLDC (16.91 dB). We can conclude that the three-core coupler (TNLDC) is presenting better values for the FOMELG parameter when compared to the two-core (DNLDC) device for the studied gates.

The TNLDC presents two extra gates, NAND and NOT which is presenting values of FOMELG (without the trivial situation, see Eq. 20) of 70.31 and 99.74 dB respectively. These extra logic gates were not observed in the DNLDC switch.

Comparing the same gates of the three and two-core NLDC we observe that the logical gates of the three-core NLDC presented a better performance than the one of the two-core NLDC considering the figure of merit FOMELG, besides the fact that is simpler to build symmetrical coupler with their cores identical in all parameters than asymmetric coupler. We believe that the use of this figure of merit will be useful in the study of the performance of logic gates to be used in communication systems.

**Acknowledgements** We thank CNPq (Conselho Nacional de Desenvolvimento Científico e Tecnológico), FINEP (Financiadora de Estudos e Projetos), CAPES (Coordenação de Aperfeiçoamento de Pessoal de Nível Superior) and FUNCAP (Fundação Cearense de Amparo a Pesquisa) for the financial support.

## References

- Agrawal, G.P.: *Nonlinear Fiber Optics*, 3rd edn. Academic Press, New York (2001). ISBN 0 12 045143 3
- Akhmediev, N., Ankiewicz, A.: Novel soliton states and bifurcation phenomena in nonlinear fiber couplers. *Phys. Rev. Lett.* **70**, 2395–2398 (1993)
- Akhmediev, N.N., Ankiewicz, A.: *Solitons—Non-Linear Pulses and Beams*, 1st edn. Optical and Quantum Electronics Series, 5. Chapman & Hall, London (1997). ISBN 0 412 75450 9
- Akhmediev, N., Soto-Crespo, J.M.: Propagation dynamics of ultrashort pulses in nonlinear fiber couplers. *Phys. Rev. E* **49**, 4519–4529 (1994)
- Atai, J., Malomed, B.A.: Stability and interactions of solitons in asymmetric dual core-optical waveguides. *Opt. Commun.* **221**, 55–62 (2003)
- Betts, R.A., Tjuguarto, T., Xue, Y.L., Chu, P.L.: Nonlinear refractive index in erbium doped optical fiber. *IEEE J. Quantum Electron.* **27**, 908–913 (1991)
- Boling, N.I., Glass, A.J., Owyong, A.: Empirical relationship for predicting nonlinear refractive index changes in optical solids. *IEEE J. Quantum Electron.* **QE-14**, 601–610 (1978)
- Buah, P.A., Rahman, B.M.A., Grattan, K.T.V.: Numerical study of soliton switching in active three-core nonlinear fiber couplers. *IEEE J. Quantum Electron.* **33**, 874–878 (1997)
- Castro, F.M., Molina, M.I., Deering, W.D.: Controlling all-optical in multicore nonlinear couplers. *Opt. Commun.* **226**, 199–204 (2003)
- Chen, Y., Snyder, A.W., Payne, D.N.: Twin core nonlinear couplers with gain and loss. *IEEE J. Quantum Electron.* **28**, 239–245 (1992)
- Chiang, K.S.: Propagation of short optical pulses in directional couplers with Kerr nonlinearity. *J. Opt. Soc. Am. B* **14**, 1437–1443 (1997a)
- Chiang, K.S.: Coupled-mode equations for pulse switching in parallel waveguides. *IEEE J. Quantum Electron.* **33**, 950–954 (1997b)
- Chu, P.L., Malomed, B.A., Peng, G.D.: switching and propagation in nonlinear fiber couplers: analytical results. *J. Opt. Soc. Am. B* **10**, 1379–1385 (1993)
- Chu, P.L., Kivshar, Y.S., Malomed, B.A., Peng, G.D., Quiroga-Teixeiro, M.L.: Soliton controlling, switching, and splitting in nonlinear fused-fiber couplers. *J. Opt. Soc. Am. B* **12**, 898–904 (1995)
- Da Silva, M.G., Sombra, A.S.B.: All-optical soliton switching in three-core nonlinear fiber couplers. *Opt. Commun.* **145**, 281–290 (1998)

- Deering, W.D., Molina, M.I., Tsironis, G.P.: Directional couplers with linear and nonlinear elements. *Appl. Phys. Lett.* **62**(20), 2471–2473 (1993)
- Donnelly, J.P., DeMeo, N.L. Jr., Ferrante, G.A.: Three-guide optical couplers in GaAs. *IEEE J. Lightwave Technol.* **LT-1**(2), 417–424 (1983)
- Fraga, W.B., Menezes, J.W.M., da Silva, M.G., Sobrinho, C.S., Sombra, A.S.B.: All optical logic gates based on an asymmetric nonlinear directional coupler. *Opt. Commun.* **262**(1), 32–37 (2006)
- Friberg, S.R., Smith, P.W.: Nonlinear optical glasses for ultrafast optical switches. *IEEE J. Quantum Electron.* **QE-23**, 2089–2094 (1987)
- Friberg, S.R., Weiner, A.M., Silberberg, Y., Sfez, B.G., Smith, P.S.: Femtosecond switching in a dual-core-fiber nonlinear coupler. *Opt. Lett.* **13**, 904–906 (1988)
- Griffin, R., Love, J.D., Lyons, P.R.A., Thorncraft, D.A., Rashleigh, S.C.: Asymmetric multimode couplers. *IEEE J. Lightwave Technol.* **9**(11), 1508–1517 (1991)
- Jensen, S.M.: The nonlinear coherent coupler. *IEEE J. Quantum Electron.* **QE-18**, 1580–1583 (1982)
- Kaup, D.K., Lakoba, T.I., Malomed, B.A.: Asymmetric solitons in mismatched dual-core optical fibers. *J. Opt. Soc. Am. B* **14**, 1199–1206 (1997)
- Kitayama, K., Wang, S.: Optical pulse compression by nonlinear coupling. *Appl. Phys. Lett.* **43**, 17–23 (1983)
- Kivshar, Y.S.: Self-localization in arrays of defocusing waveguides. *Opt. Lett.* **18**, 1147–1158 (1993)
- Lines, M.E.: Oxide glasses for fast photonic switching: a comparative study. *J. Appl. Phys.* **69**, 6876–6884 (1991)
- Lopez, F.A., Cabrera, J.M., Rueda, F.A.: *Electrooptics Phenomena, Materials and Applications*, 1st edn. Academic Press (1994). ISBN 0 12 044512 3
- Mak, W.C.K., Malomed, B.A., Chu, P.L.: Solitary waves in asymmetric coupled waveguides with quadratic nonlinearity. *Opt. Commun.* **154**, 145–151 (1998)
- Malomed, B.A., Skinner, I.M., Chu, P.L., Peng, G.D.: Symmetric and asymmetric solitons in twin core nonlinear optical fibers. *Phys. Rev. E* **53**, 4084–4091 (1996)
- Nobrega, K.Z., Sombra, A.S.B.: Optimum self phase modulation profile for nonlinear transmission recovery in twin core optical couplers with loss. *Opt. Commun.* **151**, 31–34 (1998)
- Ramos, P.M., Paiva, C.R.: All-optical pulse switching in twin-core fiber couplers with intermodal dispersion. *IEEE J. Quantum Electron.* **35**, 983–989 (1999)
- Shum, P., Chiang, K.S., Gambling, W.A.: Switching dynamics of short optical pulses in a nonlinear directional coupler. *IEEE J. Quantum Electron.* **35**, 79–83 (1999)
- Smith, P.W.: Applications of all-optical switching and logic. In: *Philosophical Transactions of the Royal Society of London. Series A, Mathematical and Physical Sciences*, vol. 313, no. 1525. *Optical Bistability, Dynamical Nonlinearity and Photonic Logic*, pp. 349–355 (1984)
- Sombra, A.S.B.: Bistable pulse collisions of the cubic-quintic nonlinear Schrödinger equation. *Opt. Commun.* **94**, 92–98 (1992)
- Stegeman, G.I., Wright, E.M.: All-optical waveguide switching. *Opt. Quantum Electron.* **22**, 95–122 (1990)
- Trillo, S., Wabnitz, S., Wright, E.M., Stegeman, G.I.: Soliton switching in fiber nonlinear directional couplers. *Opt. Lett.* **13**, 672–677 (1988)
- Trivunac-Vukovic, N.: Realization of all-optical ultrafast logic gates using triple core asymmetric nonlinear directional coupler. *J. Opt. Commun.* **22**(2), 59–63 (2001)
- Trivunac-Vukovic, N., Milovanovic, B.: Realization of full set logic gates for all-optical ultrafast switching. In: *IEEE, Telsiks 2001*, pp. 500–503 (2001)
- Valkering, T.P., De Boer, P.T., Hockstra, H.J.W.M.: Soliton dynamics in directional couplers. *Physica D* **123**, 223–234 (1998)
- Valkering, T.P., Van Honschoten, J., Hockstra, H.J.W.M.: Ultra-sharp soliton switching in a directional coupler. *Opt. Commun.* **159**, 215–220 (1999)
- Wang, Y., Liu, J.: All-fiber logical devices based on the nonlinear directional coupler. *IEEE Photonics Technol. Lett.* **11**, 72–74 (1999)
- Weiner, A.M., Silberberg, Y., Fouckhardt, H., Leaird, D.E., Saifi, M.A., Andrejco, M.J., Smith, P.W.: Use of femtosecond square pulses to avoid pulse breakup in all-optical switching. *IEEE J. Quantum Electron.* **25**, 2648–2655 (1989)
- Yang, C.C.: All-optical ultrafast logic gates that use asymmetric nonlinear directional couplers. *Opt. Lett.* **16**, 1641–1643 (1991)
- Yang, C.C., Wang, A.J.S.: Asymmetric nonlinear coupling and its applications to logic functions. *IEEE JQE* **28**, 479–487 (1992)
- Zang, D.Y., Forest, S.R.: Crystalline organic semiconductor optical directional couplers and switches using and index matching layer. *IEEE Photonics Technol. Lett.* **4**, 365–368 (1992)